CHEMISTRY
AN ASIAN JOURNAL

www.chemasianj.org

Accepted Article

Title: Ultrahigh-Content Nitrogen-doped Carbon Encapsulated Cobalt NPs as Catalyst for Oxidative Esterification of Furfural

Authors: Ting Wang, Hong Ma, Xin Liu, Yang Luo, Shujing Zhang, Yuxia Sun, Xinhong Wang, Jin Gao, and Jie Xu

To be cited as: *Chem. Asian J.* 10.1002/asia.201900099

Link to VoR: http://dx.doi.org/10.1002/asia.201900099

A Journal of

ACES Asian Chemical Editorial Society

A sister journal of Angewandte Chemie and Chemistry – A European Journal

WILEY-VCH

10.1002/asia.201900099

WILEY-VCH

Ultrahigh-Content Nitrogen-doped Carbon Encapsulated Cobalt NPs as Catalyst for Oxidative Esterification of Furfural

Ting Wang,[a,b] Hong Ma,*[b] Xin Liu,[b,c] Yang Luo,[b,c] Shujing Zhang,[b,c] Yuxia Sun,[b,c] Xinhong Wang,*[a] Jin Gao,[b] and Jie Xu [b]

Abstract: It is an attractive and challenging topic to endow the non-noble metal catalysts with high efficiency via nitrogen-doping approach. In this study, the ultrahigh-content nitrogen-doped carbon encapsulated cobalt NPs catalyst CoO_x@N-C(g) was synthesized, and detailed characterized by XRD, HRTEM, N_2-physisorption, ICP, CO_2-TPD, and XPS techniques. g-C_3N_4 nanosheets act as nitrogen source and self-sacrificing templates, giving rise to ultrahigh nitrogen content of 14.0%, much higher than those using bulk g-C_3N_4 (4.4%) via the same synthesis procedures. In consequence, CoO_x@N-C(g) exhibited the highest performance in the oxidative esterification of biomass-derived platform furfural to methylfuroate under base-free conditions, achieving 95.0% conversion and 97.1% selectivity toward methylfuroate under 0.5 MPa O_2 at 100 °C for 6 h, far exceeded those of other cobalt-based catalysts. The high efficiency of CoO_x@N-C(g) was closely related to its high ratio of pyridinic nitrogen species that may play as Lewis basic sites, as well as capacity in activation of dioxygen to superoxide radical $O_2^{\bullet-}$.

Introduction

Catalytic conversion of renewable biomass resource to bio-fuels and bio-chemicals has attracted increasing global attention.[1-2] The oxidation and oxidative esterification are involved in the most important processes for production of biomass-based products, including aldehydes, ketones, carboxylic acids, and esters, etc.[3-7] The typical functional groups conversions are the oxidation of –C–OH to –COOH and oxidative esterification of –HC=O to –COOR in platforms, such as 5-hydroxymethylfurfural (HMF) or furfural (FF).[8-13] For such processes, the transition metal catalysts always exhibit mild capacity and thus afford unsatisfactory performances, as well as easy deactivation in the presence of O_2. Therefore, the most investigated catalysts are still mainly restricted to noble metal catalysts. It is worth noting that stoichiometric or excess bases such as NaOH or K_2CO_3 could dramatically facilitate the reactions, but it also comes with high cost, high energy-consumption, environmental pollution, and hence the limited application. This raises the crucial question whether non-precious metal catalysts can simultaneously achieve high performance and stability in the presence of dioxygen under base-free conditions.

Recently, N-doped carbon-based transition-metal catalysts have been regarded as sustainable heterogeneous catalysts with unique catalytic performance even comparable with precious metal catalysts in plenty of organic reactions, electrocatalysis, and photocatalysis, etc.[14-18] It was identified that doping heterccyclic N-species in the carbon matrix could enhance the performance of Co, Fe, and Ni, etc, in term of improving the electron performance and electrical conductivity, as well as creating defects.[19-20] Particularly, basic pyridinic-N species doped in carbons could remarkably promote for the dehydrogenation steps.[21] Neverthless, these non-noble metal catalysts generally suffer from low activity when used alone.[22] To improve the catalytic activity, various basic additives are introduced in the reactions in term of activating substrates or lowering the activation energy of specific steps,[23-24] but the problems caused by base still remained.

Increasing the doping content of nitrogen in the N-doped carbon-based transition-metal catalysts seems a promising and effective approach. Up to now, several methods[25-28] have been developed, ranged from the heat-treatment with ammonia, the variation of N-containing transition metal complexes or coordination polymers as precursors, introducing extra N-complex in precursors, etc. Wiggins-Camacho et al.[26] found the nitrogen content could be directly increased to 7.4% by using ferrocene growth catalyst and m-xylene anhydrous or pyridine as the carbon source when synthesizing nitrogen doped CNT structures under Ar–NH_3 atmosphere. Vinayan et al.[27] developed a novel nitrogen doping process by pyrolysing polypyrrole coated poly(sodium 4-styrenesulfonate) functionalized graphene and achieved a nitrogen incorporation of around 7.5% with a relatively large quantity of graphitic nitrogen as well as some pyridinic nitrogen species. Lee et al.[28] revealed that variation of the amount of ethylenediamine (EDA) could increase the nitrogen content of nitrogen-doped carbon by a hydrothermal reaction. The pyridinic-N was demonstrated as the active site, and the activity of the catalysts increased with the increasing of nitrogen content. Despite the significant progresses in the design and construction of high-content N-doping materials, the concentration of the N-doping species is generally less than 10%. There remains a challenge to develop an ultrahigh-content nitrogen-doped carbon based transition metal catalyst with high ratio of pyridinic-N that is inexpensive, easy to synthesis, and environmentally friendly.[29]

Previously, our laboratory has been engaged in research of construction of functional catalytic materials and production of

[a] T. Wang, X. Wang
School of Textile and Material Engineering
Dalian Polytechnic University
Dalian 116034, P. R. China.
E-mail: qywxh@163.com
[b] T. Wang, H. Ma, X. Liu, Y. Luo, S. Zhang, Y. Sun, J. Gao, J. Xu
State Key Laboratory of Catalysis
Dalian Institute of Chemical Physics, Chinese Academy of Sciences
Dalian National Laboratory for Clean Energy
Dalian 116023, P. R. China.
E-mail: mahong@dicp.ac.cn
[c] X. Liu, Y. Luo, S. Zhang, Y. Sun
University of Chinese Academy of Sciences
Beijing 100049, P. R. China.
Supporting information for this article is given via a link at the end of the document.

chemicals from biomass-based feedstocks via catalytic methods.[21, 30-33] We found that both basic sites (pyridinic N-doped carbon species in CoO_x-N/C) and basic supports (MgO and $Mg(OH)_2$) could contribute to high catalytic performances in oxidation or oxidative esterification. On the other hand, to avoid aggregation and deactivation of nanosized metal particles with high surface energies in the aerobic oxidation conditions, we employed encapsulation strategy and demonstrated its protective effect for Co nanoparticle by N-doped graphitic carbon shells or Au nanoclusters by HY zeolite supercage.[34] These findings enlightened us to fabricate a high-efficiency and stable catalyst via increasing the N content and pyridinic ratio as well as by encapsulation strategy. In this study, we decided to choose furfural, a typical biomass-derived platform achieved from agricultural byproducts like sugarcane bagasse and corn cobs[10, 35] as model substrate to probe the oxidative esterification of –HC=O. The graphite-like carbon nitride (g-C_3N_4) nanosheets, a nitrogen-rich material, was chosen as nitrogen source and self-sacrificing template. CoO_x@N-C(g) catalyst has been synthesized, with ultra-high N content estimated to be 14.0%, showed excellent performance with high yield to methylfuroate under mild conditions without any basic additives.

Results and Discussion

Considering the exfoliated g-C_3N_4 nanosheets have highly amine groups,[22,36-37] it was performed as self-sacrificial template and compared with bulk g-C_3N_4 in term of N-content, concentration of pyridinic-N, and basicity. As illustrated in Scheme 1, the bulk g-C_3N_4 was firstly delaminated to reduce the thickness by thermal oxidation etching process in air. Compared with bulk g-C_3N_4, the FT-IR peaks of g-C_3N_4 in the region from 900 to 1800 cm^{-1} that were attributed to either trigonal C–N(–C)–C or bridging C–NH–C units became sharper, probably due to the more ordered packing of hydrogen-bond cohered long strands of polymeric melon units survived after thermal oxidation etching of bulk g-C_3N_4 (Fig. S1). The XRD patterns of g-C_3N_4 showed a peak at 27.7°, which indicated a decreased gallery distance between the basic sheets in the g-C_3N_4 nanosheets (Fig. S2).[14-15,36,38] These agree well with the significant increase in volume during the exfoliation of bulk g-C_3N_4 to g-C_3N_4 nanosheets (Fig. S3). Then, a cobalt(II) phenanthroline complex was impregnated on g-C_3N_4 nanosheets or bulk g-C_3N_4, followed by pyrolysis under a nitrogen atmosphere. The as-synthesized samples were denoted as CoO_x@N-C(g) and CoO_x@N-C(b), respectively. These two catalysts showed the similar XRD patterns (see discussion below) and core-shell structures (Figs. S4 and S5).

CoO_x@N-C(g) catalyst was carefully checked by HAADF-STEM, HRTEM, and TEM (Figs. 1a-e). The observations indicated the special core-shell nanostructure; the majority of crystalline Co NPs cores (10-50 nm) were encapsulated with thin outside shells (2-7 nm) and dispersed on CoO_x@N-C(g) (Figs 1c and d). Pyrolysis leaded Co^{2+} in $Co(phen)_2$ thermally reduced to metallic Co as evidenced by the XRD peaks at 44.2°, 51.4°, and 75.8°, accompanied by formation of cobalt oxides (36.6°, 42.2°, and 61.4° for CoO, and 18.9°, 31.2°, 36.8°, 59.3°, and 65.1° for Co_3O_4).[39] If the CoO_x@N-C(g) was immersed in 2 M HCl for 24 h, most of Co NPs remained in the N-doping graphitic carbon shells and cobalt oxides were removed as evidenced by XRD pattern of Co@N-C(g)-H (Fig. 2a). Obviously, besides with ultra-high N content, this catalyst was also endowed with a highly leaching-resistant property of Co NPs against strong acid erosion due to the protective role of shells to avoid the inner Co nanoparticles from aggregation.[25] The interlayer spacing of 0.334 nm in HRTEM image of CoO_x@N-C(g) (Fig. 1d) and the characteristic XRD peak at 26.2° (Fig. 2a) gave clear evidences that the carbons in the shells were graphitized catalyzed by Co, which was consistent with the

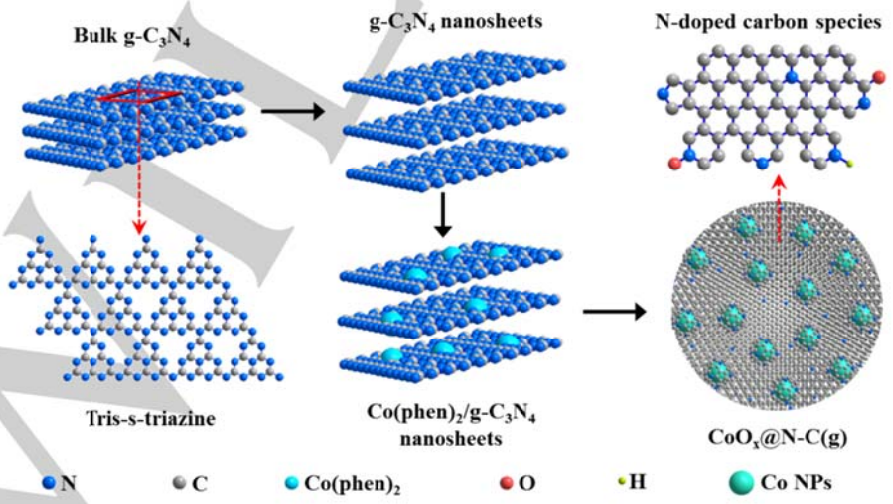

Scheme 1. Schematic illustration of the synthetic process of CoO_x@N-C(g) catalyst.

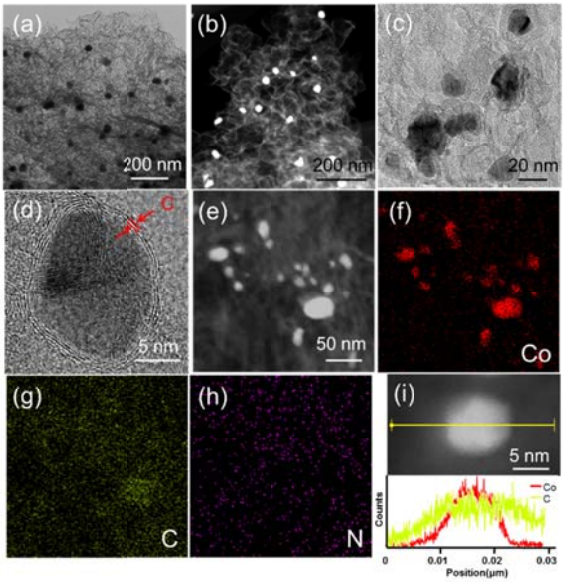

Figure 1. TEM images (a), HAADF-STEM images (b, e), HRTEM images (c, d), the corresponding EDX maps for Co (f), C (g), and N (h), and line-scan recorded along the line marked (i) for CoO_x@N-C(g).

previous literatures[25] that transition metals such as Fe, Ni, and Co in the carbon precursor could catalyze the graphitization of amorphous carbon through the solid-state transformation. Moreover, the energy-dispersive X-ray (EDX) maps and line-scan analysis for CoO_x@N-C(g) further illustrated Co, C, and N elements were highly dispersed in the carbon shell (Figs. 1e-i). These results agree with the elemental analysis that CoO_x@N-C(g) afforded an ultra-high N content of 14.0%. In contrast, only 4.4% for CoO_x@N-C(b) indicated that the exfoliated g-C_3N_4 nanosheets with reduced thickness could provide luxuriant nitrogen source, more superior to bulk g-C_3N_4. It suggested the decreased gallery distance in the g-C_3N_4 nanosheets through the thermal oxidation etching process was benefical to the nitrogen doping.

The nitrogen sorption isotherms of the CoO_x@N-C(g), CoO_x@N-C(b), and Co@N-C(g)-H catalysts showed a typical type IV isotherm with a hysteresis loop, indicating a mesoporous structure (Fig. 2b). At the same time, the surface

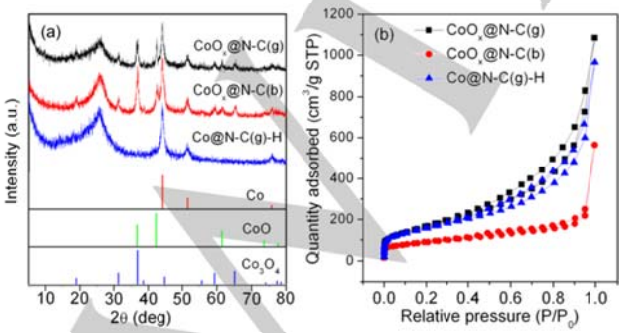

Figure 2. XRD patterns of CoO_x@N-C(g), CoO_x@N-C(b), and Co@N-C(g)-H catalysts (a), N_2 adsorption-desorption isotherms of CoO_x@N-C(g), CoO_x@N-C(b) and Co@N-C(g)-H catalysts (b).

area of CoO_x@N-C(g) (608.0 $m^2 \cdot g^{-1}$) was almost twice as large as CoO_x@N-C(b) (306.4 $m^2 \cdot g^{-1}$), presumably as a consequence of the larger surface area[15] and pore template role of g-C_3N_4 nanosheets.[22, 37] In addition, the surface of CoO_x@N-C(g)-H was 560.5 $m^2 \cdot g^{-1}$. Such a favorable textural structure is desirable for catalytic applications.

The catalytic performance of CoO_x@N-C(g) was investigated and compared with CoO_x@N-C(b), Co@N-C(g)-H, and homogeneous cobalt salts catalysts (Table 1). Exploratory experiments were performed in methanol in a 10 mL autoclave reactor. As expected, CoO_x@N-C(g) exhibted excellent activity and selectivity in the oxidative esterification of furfural under base-free conditicn, and afforded 91.1% conversion of furfural with 94.2% selectivity to methylfuroate at 100 °C under 0.5 MPa O_2 for 2 h. In contrast, CoO_x@N-C(b) only achieved 64.2% conversion, but approximate selectivity to methylfuroate (95.5%). It suggested that higher nitrogen content is in favour of oxidative esterification. For comparison purpose, the performance of CoO_x@N-C(b)-H that treated by 2 mol/L HCl was investigated, and the majority of furfural was converted to the acetal 2-(dimethoxymethyl)furan (73.7% conversion), and only a few converted to methylfuroate (13.8% selectivity). Meanwhile, the condensation between furfural and metanol occurred, with 2-(dimethoxymethyl)furan generated as the main product and methylfuroate not detected. These results revealed an important effection of nigtrogen content and its basicity on the oxidative esterification. Moreover, the homogeneous Co-based catalysts ($Co(Ac)_2$, $CoCl_2$, $Co(acac)_2$, and $Co(NO_3)_2$) showed poor catalytic performance, mainly yielding the acetal 2-(dimethoxymethyl)furan at 100 °C for 2 h. As shown in Table 1 (entries 1, 9, and 10), the conversion of furfural decreased

Table 1. Catalytic performance of various Co-based catalysts in the oxidative esterification of furfural.

Entry	Catalyst	Time (h)	Conv. (mol%)	Select.[a] (mol%)
1	CoO_x@N-C(g)	2	91.1	94.2
2	CoO_x@N-C(b)	2	64.2	95.5
3	Co@N-C(g)-H	2	73.7	13.8
4	$Co(Ac)_2$	2	0.8	n.d.
5	$CoCl_2$	2	65.6	n.d.
6	$Co(acac)_2$	2	5.3	n.d.
7	$Co(NO_3)_2$	2	70.5	n.d.
8	-	2	55.1	n.d.
9[b]	CoO_x@N-C(g)	2	43.2	94.7
10[c]	CoO_x@N-C(g)	2	69.7	94.1
11	CoO_x@N-C(g)	0.17	64.6	99.7
12	CoO_x@N-C(g)	0.5	78.6	95.2
13	CoO_x@N-C(g)	3	91.8	96.1
14	CoO_x@N-C(g)	4	92.7	98.6
15	CoO_x@N-C(g)	6	95.0	97.1

Reaction conditions: 1 mmol furfural, 60 mg CoO_x@N-C(g) catalyst (24.4 wt% Co, or equal molar Co), 5 mL of methanol, 100 °C, 0.5 MPa O_2. [a] Selectivity toward methylfuroate. [b] 20 mng CoO_x@N-C(g) catalyst. [c] 40 mg CoO_x@N-C(g) catalyst.

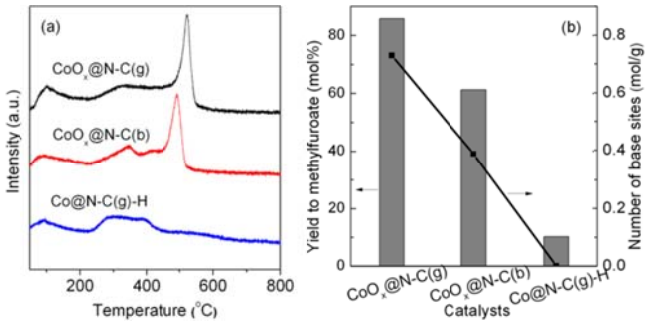

Figure 3. CO_2-TPD of CoO_x@N-C(g), CoO_x@N-C(b) and Co@N-C(g)-H catalysts (a), and the yield of these catalysts (b).

notably with the decreasing of CoO_x@N-C(g) catalyst dosage, and the optimized amount of catalyst loading was 60 mg. To obtain more information into the reaction pathway, the catalytic performance at different reaction time was studied for the CoO_x@N-C(g) catalyst (Table 1). The conversion of furfural increases rapidly at the initial 3 h (91.8% of conversion), indicating a high activity. When the time was prolonged to 4 h or 6 h, the conversion of furfural reached to 92.7% and 95.0%, respectively. The above experimental results showed that CoO_x@N-C(g) performed excellent activity and selectivity in the oxidative esterification of furfural.

Afterwards, the relationship between basicity and catalytic activity was investigated. CO_2-TPD was employed to examine the basicity of CoO_x@N-C(g), CoO_x@N-C(b), and Co@N-C(g)-H, and the results were shown in Fig. 3a. For these three samples, the broad peak between 450 °C and 550 °C was due to the strong base site,[40,41] and the amounts of strong basic sites for CoO_x@N-C(g) and CoO_x@N-C(b) were 0.73 mmol·g^{-1} and 0.39 mmol·g^{-1}, respectively. After acid treatment, such a strong base site disappeared in Co@N-C(g)-H. As shown in Fig. 3b, the yield of methylfuroate dramatically decreased in the order of CoO_x@N-C(g) > CoO_x@N-C(b) > Co@N-C(g)-H, from 85.8% to 61.3% and 10.2%, respectively. It agreed well with the order of amounts of strong base sites of the catalysts. The deconvoluted results manifested that the decrease of the amounts of strong base sites contributed to the distinctly declined activity of the three catalysts. The discrimination in total content N content of the samples may be one of the reasons for different amount of base sites, such as the total N content of CoO_x@N-C(g) and CoO_x@N-C(b) were 14.0 % and 4.4 %, respectively (Table S1). It is noteworthy that, in spite of the total N content of Co@N-C(g)-H was as high as 11.5 %, it only achieved a low activity in the oxidative esterification, indicating that the acid treatment of CoO_x@N-C(g) caused the decrease of the amount of basic sites. In previous studies, furan, pyrrole, and thiofuran derivative heterocyclic compounds can be polymerized via oxidative dehydrogenation under acidic conditions or using acidic catalysts[42-45]. In our case, the oxidative esterification of furfural was performed without any alkali or acid additives, avoiding the polymerization of furfural. It indicated the basicity in CoO_x@N-C(g) catalyst played a crucial role in promoting the oxidative esterification process.

To determine the origin of basic sites, CoO_x@N-C(g), CoO_x@N-C(b), and Co@N-C(g)-H catalysts were studied by X-ray photoelectron spectroscopy (XPS), and the results were shown in Fig. 4. For both CoO_x@N-C(g) and CoO_x@N-C(b) catalysts, their N1s XPS spectra displayed four over-lapped peaks at 398.5 eV (pyridinic N and pyridinic N bonded to Co), 400.0 eV (pyrrolic N or pyridonic N), 400.8 eV (graphic N or pyridinic N$^+$-H), and 402.0-403.2 eV (pyridine N-oxide), which were denoted as N1, N2, N3 and N4, respectively.[46-49] These N-species have been demonstrated to be arisen from a decomposition of phenanthroline ligand and g-C_3N_4, and the subsequent doping in carbon process at 800 °C under N_2. As evidenced in previously reported literatures,[50] pyridinic-N could behave as Lewis bases and denote lone pair of electrons that are not delocalized in the aromatic p system, while other five species including pyridinic N bonded to Co, pyrrolic N, graphic N, pyridinic N$^+$-H, and pyridine N-oxide lack such basicity.

Therefore, the variation in the peak at 398.5 eV during acid-treatment was due to the protonation of pyridinic N to pyridinic N$^+$-H, and change in the peak at 400.8 eV was related to pyridinic N$^+$-H.[20] It was noteworthy that the pyridinic N content of CoO_x@N-C(g)-H was decreased by 10.5% compared to CoO_x@N-C(g), close to the increased content of pyridinic N$^+$-H (10.6%) (Table S1). Accordingly, the N1 peak shifted toward higher binding energy, reflecting a decrease of pyridinic N (pyridinic N bonded to Co was excluded). In the case of CoO_x@N-C(b), we also observed an obvious lower ratio of N1 peak and a higher ratio of N3 peak, which agreed well with the previous literature.[41] Combined the quantitative XPS analysis and CO_2-desorption results, we deduced that the pyridinic N may create the strong Lewis basic sites, which may be dramatically decreased due to the protonation of N in HCl treatment.

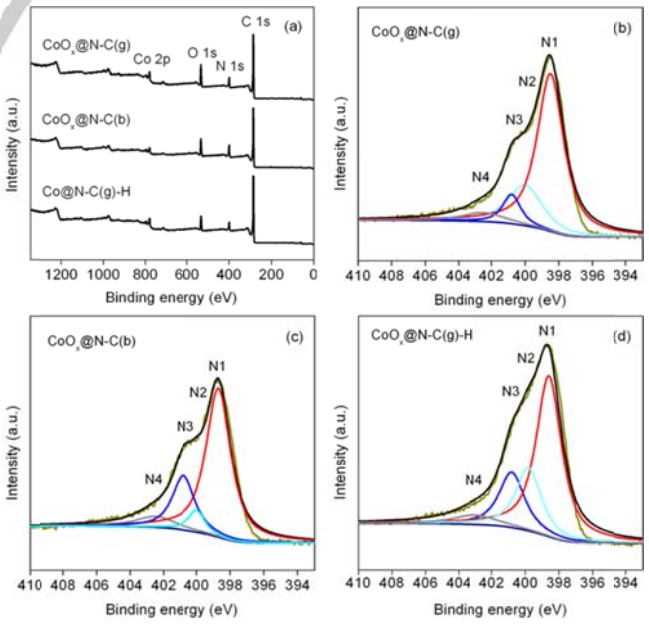

Figure 4. XPS spectra of three samples (a) and high-resolution XPS spectra of N1s for CoO_x@N-C(g) (b), CoO_x@N-C(b) (c) and Co@N-C(g)-H (d).

Table 2. Catalytic performances of various Co-based catalysts in the oxidative esterification of furfural.

entry	Catalyst	Additives	Conv. (mol%)	Select.[a] (mol%)
1	Co@N-C(g)-H	K_2CO_3	93.5	95.4
2	CoO_x@N-C(g)	NaCl	62.2	97.9
3	CoO_x@N-C(g)	PBQ	24.6	95.1
4	Co@N-C(g)-H	PBQ	79.2	5.8
5	Co@N-C(g)-H	K_2CO_3/PBQ	25.6	96.0
6[b]	CoO_x@N-C(g)	-	10.9	96.1

Reaction conditions: 1 mmol furfural, 60 mg CoO_x@N-C(g) catalyst (24.4 wt% Co, or equal molar Co), 5 mL of methanol, 100 °C, 0.5 MPa O_2, 2 h. [a] Selectivity toward methylfuroate. [b] N_2 atmosphere.

To gain more insight into the role of basic pyridinic-N species and reaction process, we investigated the catalytic performance of Co@N-C(g)-H in the addition of K_2CO_3 or NaCl in the oxidative esterification of furfural in methanol under 0.5 MPa O_2 at 100 °C for 2 h. As mentioned above, Co@N-C(g)-H alone mainly gave 2-(dimethoxymethyl)furan, an acetal product via the condensation between furfural and methanol. If K_2CO_3 was introduced into the reaction with Co@N-C(g)-H, the catalytic performance recovered with 93.5% conversion of furfural and 95.4% selectivity towards methylfuroate (Table 2, entry 1). This supposed that pyridinic N^+-H may be recovered to pyridinic N by K_2CO_3. To exclude the potential role of the residual Cl^- from the HCl treatment, NaCl (0.5 mmol) was introduced into the reaction using CoO_x@N-C(g). The selectivity to methylfuroate remained high (97.9%) with conversion decreased from 91.1% to 62.2% (Table 2, entry 2), indicating that Cl^- could not alter the reaction pathway, and the partial loss of catalytic activity may be its affection on the metal centers as illustrated by our previous studies.[30] Therefore, all the above implied that the pyridinic N may play a similar role to K_2CO_3. As demonstrated in our previous studies,[31] Co NPs encapsulated with N-doped graphitic carbon shells could activate molecular oxygen to generate superoxide radical ($O_2^{\bullet-}$), an activated oxygen species that was responsible for the oxidative conversion of lignin-derived alcohols, the availability of such capacity of CoO_x@N-C(g) was further investigated. p-Benzoquinone (PBQ, 0.2 mmol), a specific radical quencher to inhibit the generation of $O_2^{\bullet-}$, was added to the reaction system with CoO_x@N-C(g) (Table 2, entry 3). The conversion of furfural dramatically decreased to 24.6% with selectivity towards methylfuroate retained (95.1%), indicating that PBQ suppressed the activity of CoO_x@N-C(g) catalyst by quenching $O_2^{\bullet-}$, but could not change the pathway. When adding PBQ to Co@N-C(g)-H, condensation remained the dominant reaction. However, the introducing of both PBQ and K_2CO_3 could regulate the reaction to follow the oxidative esterification pathway, with 96.0% selectivity to methylfroate (Table 2, entry 5). It also illustrated that the pyridinic N may contribute to the oxidative esterification like K_2CO_3 in this reaction despite the activity suppresed. Furthermore, a set of control experiments on trapping active species by the trapping agent butylated hydroxytoluene (BHT) were performed (Fig. 5). $O^{2\bullet-}$ species was captured by BHT when using CoO_x@N-C(g) as evidenced by the detection of BHT-OOH by GC-MS (Fig. 5).

The stability of the CoO_x@N-C(g) catalyst was investigated for the oxidation esterification of furfural (Fig. 6). The CoO_x@N-C(g) catalyst retained its activity for at least three recycling runs, with only a slight attenuation of activity, which was mainly attributed to the loss of catalyst du ring washing and filtration. In addition, a reduction process was indispensible to regenerate the catalyst, where the spent CoO_x@N-C(g) catalyst was reduced at 400 °C for 2 h under a H_2 atmosphere. Otherwise, it only gave poor performance at the recycling test. The exact

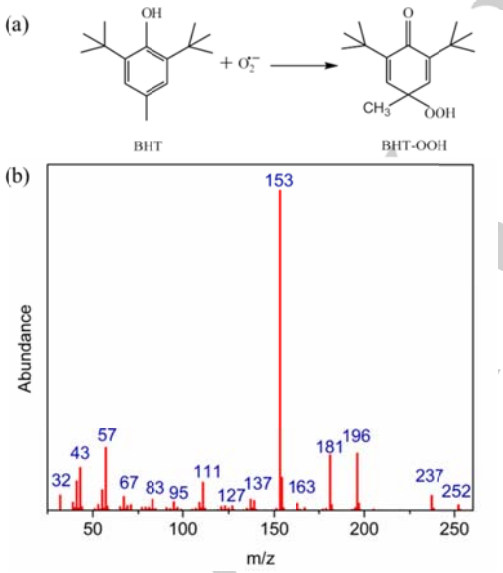

Figure 5. The superoxide radical anion capture experiment with BHT converting to BHT-OOH (a) and the mass spectrum of the captured species BHT-OOH (b).

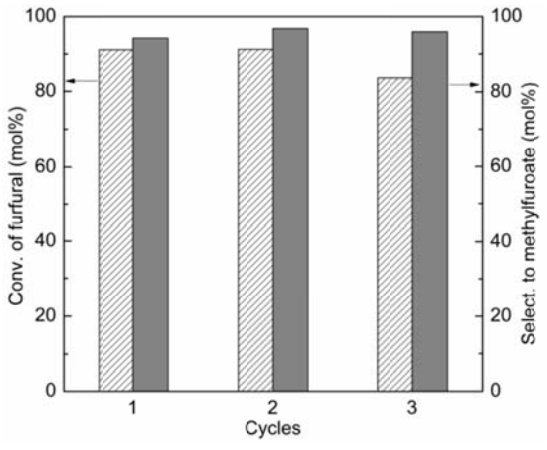

Figure 6. Recycling experiments of CoO_x@N-C(g). Reaction conditions: 1 mmol furfural, 60 mg CoO_x@N-C(g) catalyst, 5 mL of methanol, 100 °C, 0.5 MPa O_2, 2 h.

10.1002/asia.201900099

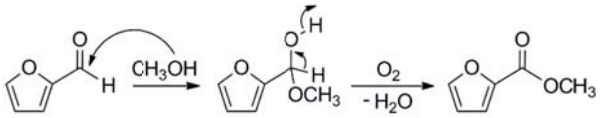

Scheme 2. Proposed mechanism of oxidative esterification of furfural with methanol catalyzed by CoO_x@N-C(g).

identity of active site in CoO_x@N-C(g) catalyst is still unclear, and need further study. Neverthless, the CoO_x@N-C(g) catalyst presented stability and can be reused in the oxidation of furfural to methylfuroate.

The proposed mechanism of oxidative esterification of furfural catalyzed by CoO_x@N-C(g) was illustrated in Scheme 2. Due to the high stability and the high ratio of pyridinic-N species (Lewis basic sites) of CoO_x@N-C(g) catalyst, the reaction system could keep neutral during the reaction process. Under such environment and in the presence of dioxygen, furfural converted into the intermediate hemiacetal via the condensation with methanol, and subsequently underwent a dehydrogenation to form methylfuroate.

Conclusions

In summary, we designed and synthesized an ultrahigh-content nitrogen-doped carbon encapsulated cobalt NPs catalyst CoO_x@N-C(g) via impregnation and pyrolysis of a cobalt(II) phenanthroline complex using g-C_3N_4 nanosheets as nitrogen source and self-sacrificing template. CoO_x@N-C(g) exhibited superior efficiency to other cobalt-based catalysts in the oxidative esterification of biomass-derived platform furfural under base-free conditions, achieving 95.0% conversion and 97.1% selectivity to methylfuroate under 0.5 MPa O_2 at 100 °C for 6 h. The CO_2-TPD measurements, element anaysis, and quantitative XPS analysis indicated the exfoliated g-C_3N_4 nanosheets could result in an ultra-high N content of 14.0%, with higher amounts of basic sites and ratio of pyridinic-N increased. As revealed by experimental results, the CoO_x@N-C(g) catalyst was endowed with capacity in activating dioxygen, and the generation of superoxide radical $O_2^{\cdot-}$ was evidenced by the quenching experiments and radical capturement. In addition, pyridinic-N may play a base role like K_2CO_3, and thus these unique properties promtes the high efficiency even without the requirement for a basic additive in the oxidative oxidation. Here, it opens new opportunities for designing non-precious metal catalysts as well as dioxygen activation, by using g-C_3N_4 nanosheets as sacrificed support and nitrogen source to achieve ultra-high content of doped nitrogen in carbon, thereby providing a simple and efficient approach for the oxidative esterification of biomass-derived hydroxyl compounds.

Experimental Section

Chemicals and materials. All reagents and chemicals used were of analytical grade unless otherwise specified. Furfural, melamine, ethanol, activated carbon, and 1, 10-phenanthroline were obtained from Aladdin Chemistry Co. Ltd. (Shanghai, China). Methanol was obtained from Kermel Chemical Reagent Development Center (Tianjin, China). Cobalt acetate tetrahydrate was from Sinopharm Chemical Reagent Co. Ltd.

Catalysts preparation. In this work, the bulk g-C_3N_4 was synthesized according to a reported method with some modifications.[15] Bulk g-C_3N_4 was first obtained by thermal polymerization of melamine at 550 °C for 4 h at a rate of 2 °C·min^{-1}. Then, the bulk g-C_3N_4 were delaminated to reduce the thickness by thermal oxidation etching process in air at 550 °C for 2 h at a rate of 5 °C·min^{-1}, thus yielding nanosheets.
The CoO_x@N-C(g) catalyst was synthesized according to a reported method with some modifications.[30] 1,10-Phenanthroline (180.2 mg, 1.0 mmol) and cobalt acetate tetrahydrate (124.5 mg, 0.5 mmol) were dissolved in 50 mL of ethanol and stirred for 30 min at room temperature. Then, 695.3 mg of g-C_3N_4 nanosheets were added to the solution, and the solution was refluxed for 4 h under magnetic stirring. After solvent was removed, the solid powder was then dried at 80 °C for 12 h. Then, the dried mixture was placed in a quartz tube furnace and heated to 800 °C for 2 h at a rate of 25 °C·min^{-1} under a nitrogen atmosphere. For comparison, cobalt-based catalysts was prepared by a similar method, a $Co(phen)_2(OAc)_2$ complex precursor was supported on bulk g-C_3N_4, then calcination and the resulting sample was denoted as CoO_x@N-C(b).

Catalyst characterization. The samples were analyzed by X-ray powder diffraction (XRD) on a Rigaku D/Max 2500/PC powder diffractometer with Cu K_α radiation (λ = 0.15418 nm) at 40 kV and 200 mA at a scanning rate of 5 °·min^{-1}. Transmission electron microscopy (TEM) images were obtained using a JEOL JEM-2000EX electron microscopy with samples deposited on a carbon polymer supported copper grid. High-resolution transmission election microscopy (HRTEM) observations were carried out on a JEM-2100F microscope operated at an acceleration voltage of 200 KV. XPS measurements were performed on a Thermo ESCALAB 250Xi using a Mg K_α (1253.6 eV) radiation source and a chamber pressure lower than 0.5 × 1 × 1 kPa. Inductively coupled plasma optical emission spectrometry (ICP-OES) using a Perkin Elmer ICP-OES 7300DV was used to determine the cobalt content. A carbon/sulfur analyzer (EMIA-8100, HORIBA) and oxygen/nitrogen/hydrogen analyzer (EMGA-930, HORIBA) were used to determine the carbon and nitrogen contents, respectively.

Oxidative esterification of furfural under base-free conditions. The catalytic activity of catalysts for the oxidation of furfural was carried out in a 10-mL Teflon lined stainless steel autoclave. Typically, 1 mmol of furfural, 60 mg of CoO_x@N-C(g) (24.4% mass fraction, 0.25 mmol of Co), and 5 mL of methanol were loaded into the autoclave. After the autoclave was purged 3 times with oxygen gas, the mixture was stirred under 0.5 bar of oxygen at 100 °C for 2 h. During the reaction, the pressure was maintained by supplying oxygen. Finally, the reaction mixture was diluted with methanol and

analyzed using an Agilent gas chromatograph (GC 7890D) equipped with a flame ionization detector (FID) and Agilent GC/MS 6890-5973. The conversion and selectivity towards methylfuroate were evaluated by the internal standard method using *n*-dodecane as the internal standard.

Acknowledgements

This work was supported by National Natural Science Foundation of China (21790331, 21872138, and 21690084) and the Strategic Priority Research Program of Chinese Academy of Sciences (Grant No: XDA21030400).

Keywords: Cobalt • Furfural • g-C_3N_4 nanosheets • Nitrogen-doped carbon • Oxidative esterification

[1] P. Lanzafame, G. Centi, S. Perathoner, *Chem. Soc. Rev.* **2014,** *43*, 7562-7580.
[2] J. C. Serrano-Ruiz, R. Luque, A. Sepulveda-Escribano, *Chem. Soc. Rev.* **2011,** *40*, 5266-5281.
[3] L. Hu, L. Lin, Z. Wu, S. Y. Zhou, S. J. Liu, *Renew. Sust. Energ. Rev.* **2017,** *74*, 230-257.
[4] T. L. Lohr, Z. Li, T. J. Marks, *Accounts Chem. Res.* **2016,** *49*, 824-834.
[5] A. Corma, S. Iborra, A. Velty, *Chem. Rev.* **2007,** *107*, 2411-2502.
[6] M. Y. Zhang, J. J. Shi, W. S. Ning, Z. Y. Hou, *Catal. Today* **2017,** *298*, 234-240.
[7] M. Y. Zhang, Y. Y. Sun, J. J. Shi, W. S. Ning, Z. Y. Hou, *Chin. J. Catal.* **2017,** *38*, 537-544.
[8] B. Liu, Y. S. Ren, Z. H. Zhang, *Green Chem.* **2015,** *17*, 1610-1617.
[9] X. L. Tong, Z. H. Liu, L. H. Yu, Y. D. Li, *Chem. Commun.* **2015,** *51*, 3674-3677.
[10] E. Taarning, I. S. Nielsen, K. Egeblad, R. Madsen, C. H. Christensen, *ChemSusChem* **2008,** *1*, 75-78.
[11] J. J. Meng, M. Gao, Y. P. Wei, W. Q. Zhang, *Chem. Asian J.* **2012,** *7*, 872-875.
[12] J. F. Nie, J. H. Xie, H. C. Liu, *J. Catal.* **2013,** *301*, 83-91.
[13] J. F. Nie, H. C. Liu, *J. Catal.* **2014,** *316*, 57-66.
[14] P. Niu, L. L. Zhang, G. Liu, H. M. Cheng, *Adv. Funct. Mater.* **2012,** *22*, 4763-4770.
[15] F. A. Westerhaus, R. V. Jagadeesh, G. Wienhofer, M. M. Pohl, J. Radnik, A. E. Surkus, J. Rabeah, K. Junge, H. Junge, M. Nielsen, A. Bruckner, M. Beller, *Nature Chem.* **2013,** *5*, 537-543.
[16] Y. Fan, P. F. Liu, Z. Y. Huang, T. W. Jiang, K. L. Yao, R. Han, *J. Power Sources* **2015,** *280*, 30-38.
[17] J. Deng, H. J. Song, M. S. Cui, Y. P. Du, Y. Fu, *ChemSusChem* **2014,** *7*, 3334-3340.
[18] J. X. Han, F. F. Gu, Y. C. Li, *Chem. Asian J.* **2016,** *11*, 2594-2601.
[19] L. Jiang, L. Mi, K. Wang, Y. F. Wu, Y. Li, A. R. Liu, Y. J. Zhang, Z. Hu, S. Q. Liu, *ACS Appl. Mater. Inter.* **2017,** *9*, 31968-31976.
[20] K. N. Wood, R. O'Hayre, S. Pylypenko, *Energ. Environ. Sci.* **2014,** *7*, 1212-1249.
[21] Y. X. Sun, H. Ma, X. Q. Jia, J. P. Ma, Y. Luo, J. Gao, J. Xu, *ChemCatChem* **2016,** *8*, 2907-2911.
[22] H. Su, K. X. Zhang, B. Zhang, H. H. Wang, Q. Y. Yu, X. H. Li, M. Antonietti, J. S. Chen, *J. Am. Chem. Soc.* **2017,** *139*, 811-818.
[23] R. V. Jagadeesh, H. Junge, M. M. Pohl, J. Radnik, A. Bruckner, M. Beller, *J. Am. Chem. Soc.* **2013,** *135*, 10776-10782.
[24] Y. X. Zhou, Y. Z. Chen, L. N. Cao, J. L. Lu, H. L. Jiang, *Chem. Commun.* **2015,** *51*, 8292-8295.
[25] M. Lefevre, E. Proietti, F. Jaouen, J. P. Dodelet, *Science* **2009,** *324*, 71-74.
[26] J. D. Wiggins-Camacho, K. J. Stevenson, *J. Phys. Chem. C* **2009,** *113*, 19082-19090.
[27] B. P. Vinayan, S. Ramaprabhu, *J. Mater. Chem. A* **2013,** *1*, 3865-3871.
[28] H. Lee, H. Kim, *J. Appl. Electrochem.* **2013,** *43*, 553-557.
[29] H. Su, K. X. Zhang, B. Zhang, H. H. Wang, Q. Y. Yu, X. H. Li, M. Antonietti, J. S. Chen, *J. Am. Chem. Soc.* **2017,** *139*, 811-818.
[30] N. Huo, H. Ma, X. H. Wang, T. L. Wang, G. Wang, T. Wang, L. L. Hou, J. Gao, J. Xu, *Chin. J. Catal.* **2017,** *38*, 1148-1154.
[31] Y. X. Sun, H. Ma, Y. J. Luo, S. Zhang, J. Gao, J. Xu, *Chem. Eur. J.* **2018,** *24*, 4653-4661.
[32] T. L. Wang, H. Ma, J. Gao, X. H. Wang, Y. X. Sun, Y. Luo, S. J. Zhang J. Xu, *Chem. Asian J.* **2017,** *12*, 2790-2793.
[33] X. Q. Jia, J. P. Ma, F. Xia, Y. M. Xu, J. Gao, J. Xu, *Nature Commun.* **2018,** *9*, 933.
[34] J. Y. Cai, H. Ma, J. J. Zhang, Z. T. Du, Y. Z. Huang, J. Gao, J. Xu, *Chin. J. Catal.* **2014,** *35*, 1653-1660.
[35] X. D. Li, P. Jia, T. F. Wang, *ACS Catal.* **2016,** *6*, 7621-7640.
[36] X. F. Chen, L. G. Zhang, B. Zhang, X. C. Guo, X. D. Mu, *Sci. Rep-Uk* **2016,** *6*.
[37] H. Park, D. H. Youn, J. Y. Kim, W. Y. Kim, Y. H. Choi, Y. H. Lee, S. H. Choi, J. S. Lee, *ChemCatChem* **2015,** *7*, 3488-3494.
[38] L. Corp Kathryn and W. Schlenker Cody, *J. Am. Chem. Soc.* **2017**, 139, 7904-7912.
[39] Z. Y. Wu, P. Chen, Q. S. Wu, L. F. Yang, Z. Pan, Q. Wang, *Nano. Energy* **2014,** *8*, 118-125.
[40] L. Gong, L. B. Sun, Y. H. Sun, T. T. Li, X. Q. Liu, *J. Phys. Chem. C* **2011,** *115*, 11633-11640.
[41] S. Shi, C. Chen, M. Wang, J. P. Ma, J. Gao. J. Xu. *Catal. Sci. Technol.* **2014,** *4*, 3606-3610. [20] K. N. Wood, R. O'Hayre, S. Pylypenko, *Energ. Environ. Sci.* **2014,** *7*, 1212-1249.
[42] X. G. Li, Q. F. Lü, M. R. Huang, *Small* **2008**, *4*, 1201-1209.
[43] X. G. Li, J. Li, M. R. Huang, *Chem. Eur. J.* **2009**, *15*, 6446-6455.
[44] X. G. Li, J. Li, M. R. Huang, Y. Z. Liao, Y. G. Lu, *J. Phys. Chem. C* **2010**, *114*, 19244-19255.
[45] X. G. Li, Y. Kang, M. R. Huang, *J. Comb. Chem.* **2006**, *8*, 670-678.
[46] Y. Ito, C. Christodoulou, M. V. Nardi, N. Koch, M. Klaui, H. Sachdev, K. Mullen, *J. Am. Chem. Soc.* **2015,** *137*, 7678-7685.
[47] R. Arrigo, M. Havecker, S. Wrabetz, R. Blume, M. Lerch, J. McGregor, E. P. J. Parrott, J. A. Zeitler, L. F. Gladden, A. Knop-Gericke, R. Schlogl, D. S. Su, *J. Am. Chem. Soc.* **2010,** *132*, 9616-9630.
[48] P. Chen, T. Y. Xiao, Y. H. Qian, S. S. Li, S. H. Yu, *Adv. Mater.* **2013,** *25*, 3192-3196.
[49] R. Arrigo, M. Havecker, R. Schlogl, D. S. Su, *Chem. Commun.* **2008,** *0*, 4891-4893.
[50] D. H. Guo, R. Shibuya, C. Akiba, S. Saji, T. Kondo, J. Nakamura, *Science* **2016**, *16*, 361-365.

10.1002/asia.201900099

COMMUNICATION

A ultrahigh-content nitrogen-doped carbon encapsulated cobalt NPs catalyst CoO_x@N-C(g) exhibited the highest performance in the oxidative esterification of biomass-derived platform furfural under base-free conditions, achieving 95.0% conversion and 97.1% selectivity toward methylfuroate under 0.5 MPa O_2 at 100 °C for 6 h.

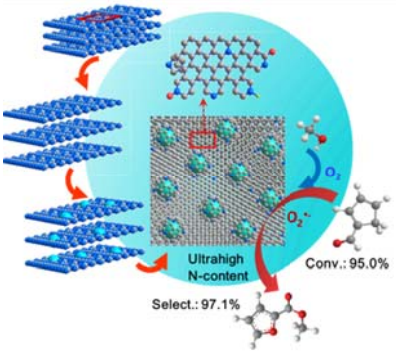

T. Wang, H. Ma, X. Liu, Y. Luo, S. Zhang, Y. Sun, X. Wang*, J. Gao, J. Xu*

Page No. – Page No.

Ultrahigh-Content Nitrogen-doped Carbon Encapsulated Cobalt NPs as Catalyst for Oxidative Esterification of Furfural